Sliding Mode Trim and Attitude Control of a 2-DOF Rigid-Rotor Helicopter Model

Heon-Sul Jeong* and Se-Myong Chang**
School of Mechanical Engineering
Kunsan National University, Kunsan-shi, Chonbuk, Korea 573-701

Jin-Sung Park***
Hydraulic Power Transmission Research Laboratory
Korea Institute of Machinery and Materials, Yusung-gu, Taejon, Korea 305-600

Abstract

An experimental control system is proposed for the attitude control of a simplified 2-DOF helicopter model. The main rotor is a rigid one, and the fuselage is simply supported by a fixed hinge point where the longitudinal motion is decoupled from the lateral one since the translations and the rolling rotation are completely removed. The yaw trim of the helicopter is performed with a tail rotor, by which the azimuthal attitude can be adjusted on the rotatable post in the yaw direction. The robust sliding mode control tracking a given attitude angle is proposed based on the flight dynamics. A pitch damper is inserted for the control of pitching angle while the compensator to reaction torque is used for the control of azimuth angle. Several parameters of the system are selected through experiments. The results shows that the proposed control method effectively counteracts nonlinear perturbations such as main rotor disturbance, undesirable chattering, and high frequency dynamics.

Key Word : 2-DOF helicopter model, Rigid rotor, Pitch damper, Torque compensator

Introduction

The flight dynamics of a rotary-wing aircraft is so complex that many researchers have investigated on the various topics of the attitude control of a helicopter. Their studies are primarily focused on the blade dynamics, rotor dynamics, and trim control in the hovering or forward flight mode (Prouty, 1986; Newman, 1994).

So far many researchers have sticked to design the control system based on linear theories. Such techniques are listed as linear quadratic regulator design, LQG/LTR controller, eigenvalue-eigenvector assignment, and H_∞ optimal control: see the review of Parry and Murray-Smith (1985) or Mannes et al (1990) in detail. Postlethwaite and Walker (1994) applied H_∞ robust control theory, and Sugeno applied fuzzy control theory, but overall helicopter control theories have been so conservative ones until now. To remove some cross coupling, for example, nonlinearity, uncertainty of parameter, dynamics of blades, and ground effect, we design a robust controller based on the slide mode theory in this paper.

In the real helicopter dynamics and control, the total degree of freedom (DOF) is six: three translations and three rotations (pitching, rolling, and yawing), so the main rotor experiences very

* Professor, Automatic Control Laboratory
E-mail : hsjeong@kunsan.ac.kr, TEL : 063-469-4723, FAX : 063-469-4727
** Assistant Professor, Wave Engineering Laboratory
*** Research Engineer

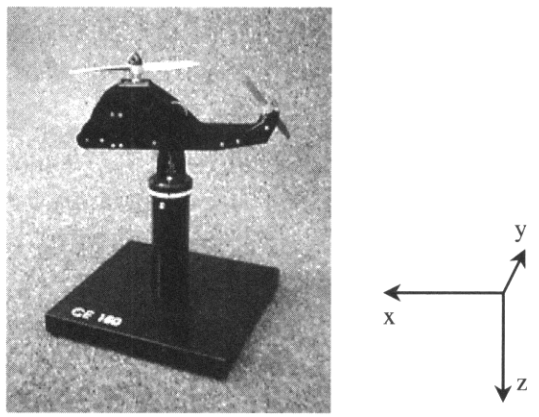

Fig. 1. Photograph of the 2-DOF model helicopter

complex coupling among those various parameters. In this paper, a reduced form of the simplified experimental model is introduced for the analysis of isolated pitch and yaw control. This 2-DOF system with main and tail rotor, powered by each electric motor respectively, is hinged at the point located on the yawing post near the center of gravity.

Therefore, the objective of this study is the benchmark test of our slide-mode control algorithm experimentally to the simplified model. The equations of flight dynamics for this reduced DOF problem are derived in the following section, and in the next, various control methods like the damping law of pitch motion, the torque compensator for azimuth reaction, and the robust controller are explained in the sequence. The experimental setup of the present apparatus is given with the identified parameters, and in the last section some discussion is presented as conclusion also with some physical interpretation.

Dynamics of Reduced DOF Helicopter

The photograph of the experimental model is shown in Fig. 1 and its conceptual sketch is given in Fig. 2. The following dynamics equations are derived on the body-fixed coordinate system, including aerodynamic and gravitational moments. The flow velocity induced by each rotor is assumed to be uniform, and the transient motion from unsteady aerodynamic effects are ignored for the equilibrium state.

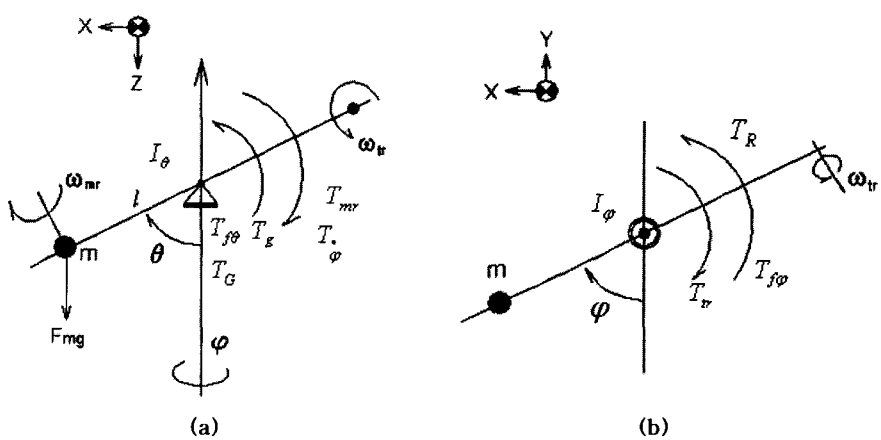

Fig. 2. Schematic sketch: (a) longitudinal (side view), (b) lateral (top view)

The Dynamics of Fuselage

In Fig. 2 the elevation (pitch) angle θ is the solution of the following second-order dynamics:

$$I_\theta \ddot{\theta} = T_{mr} - T_{f\theta} - T_g + T_{\dot{\varphi}} - T_G \tag{1}$$

where each torque contribution is main rotor T_{mr}, friction $T_{f\theta}$, gravitational T_g, centrifugal $T_{\dot{\varphi}}$, and gyroscopic T_G as follows:

$$\begin{aligned} T_{f\theta} &= B_\theta \dot{\theta} + C_\theta \, sign(\dot{\theta}) \\ T_g &= mgl \sin\theta \\ T_{\dot{\varphi}} &= \frac{1}{2} m (l\dot{\varphi})^2 \sin 2\theta \\ T_G &= K_{G\dot{\varphi}\omega_{mr}} \cos\theta \end{aligned} \tag{2}$$

where B is viscous friction coefficient, and C is Coulumb's friction torque. Additional effect of reaction torque of tail rotor is neglected here.

The azimuth (yaw) angle dynamics is

$$I_\varphi \ddot{\varphi} = T_{tr} - T_{f\varphi} - T_R \tag{3}$$

where each torque contribution is tail rotor T_{tr}, friction $T_{f\varphi}$, reaction from the main rotor T_R. Note that the inertia I_φ changes with respect to θ proportional to $I_z \sin\theta$.

The Dynamics of Blades and Electric Motors

In the similar way, the blades are governed by the following dynamics:

$$I_{ir} \dot{\omega}_{ir} = T_{Mi} - T_{fi} - T_{ai}, \quad i = m, t \tag{4}$$

where the subscript m and t denote main and tail rotor, respectively. The input voltage is V, and ω_{ir} is the rotational speed of each rotor. The torque components are motor driving T_M, friction T_f, and air resistance (by drag force in the blade elements) T_a.

$$\begin{aligned} T_{Mi} &= K_{Mi} \frac{V_i - K_{bi}\omega_{ir}}{R_i} \\ T_{fi} &= B_{ir} + C_{ir} sign(\omega_{ir}), \qquad i = m, t \\ T_{ai} &= B_{ai}\omega_{ir} + D_{ai}\omega_{ir}^2 \, sign(\omega_{ir}) \end{aligned} \tag{5}$$

where K_M is motor torque coefficient, K_{bi} is back-emf constant, and R is the coil resistance. The motor torque is proportional to the input power. The last one in Eq. (5) indicates aerodynamic physics. The first term is torque derived by the drag in the laminar flow regime, but the second is the effect of profile and induced drag in the high sectional Reynolds number.

By the momentum (or actuating disc) theory and blade element method, the rotor torque to produce thrust is

$$T_{ir} = K_{ai}\omega_{ir}^2 \, sign(\omega_{ir}) \tag{6}$$

The rotor power is the third power of rotational speed, so the torque is proportional to the square of rotor angular speed in the above equation.

Design of Attitude Controller

The dynamics equations show several nonlinear cross-coupled terms, and also there may be possible errors due to the high-order dynamics excluded in the theoretical model or the unsteady transient flow physics. Consequently, the robust control method based on sliding mode theory is proposed here for the closed-loop feedback control.

The Damping Law of Pitch Motion

In the hovering, the blades with an ideal twist produces the uniform flow with a thrust proportional to disc area and the square of induced velocity. In the climbing or descending, the thrust is changed from that of hovering, and therefore the difference makes a disturbance impeding smooth pitching motion in our system. Especially, in the descending, there is the unstable flow area which cannot be simply predicted, called vortex ring region or auto-rotation. The input thrust from main rotor is changed in a nonlinear way, and the controller must damp the unexpected torque variation. The damping law of pitch motion is

$$V_{d\theta} = K_{d\theta}\left(\frac{\dot{\theta}}{\omega_{mr}}\right)^2 sign\left(\dot{\theta}\right) \tag{7}$$

The Pitch Controller for Elevation Angle

Substituting Eq. (6) into Eq. (1), we get

$$I_\theta \ddot{\theta} = -T_g - T_{f\theta} + T_\varphi - T_G + K_{am}\omega_{mr}^2 sign\left(\omega_{mr}\right) \tag{8}$$

Substituting Eq. (5) into Eq. (4) for $i = m$ (main rotor),

$$I_{mr}\dot{\omega}_{mr} = -T_{fm} - T_{am} - K_{Mm}\frac{K_{bm}}{R_m}\omega_{mr} + \frac{K_{Mm}}{R_m}V_m \tag{9}$$

The output of this system is an elevation angle θ, and V_m, the voltage of main rotor shaft motor becomes the input. By integrating Eq. (9), for example, we can fix the source term in the right hand side of Eq. (8) using ω_{mr} to integrate to finally the instant elevation.

Then we use a sliding dynamics technique (Jeong and Utkin, 1999). To ease the design as well as gain tuning procedure, the sliding surface is selected as follows. At first, consider the main rotor speed as a control input of the dynamics Eq. (9). For the sequential design, a sliding function s^θ is selected as

$$\begin{aligned} s^\theta &= \dot{\epsilon}^\theta + k_1^\theta \epsilon^\theta \\ \epsilon^\theta &= \theta - \theta_d \end{aligned} \tag{10}$$

where d denotes the desired one or given command. The sliding function can be enforced to the zero level by use of a conventional discontinuous switching function. However, the rotational speed of main rotor is implicitly given in Eq. (9), not a closed-form, and moreover the dynamic delay of blades due to the inertia of rotor may degrade the system performance given in Eq. (10). Therefore, we take sliding function once more as follows.

$$\sigma^\theta = \dot{s}^\theta + k_2^\theta s^\theta = \ddot{\epsilon}^\theta + (k_1^\theta + k_2^\theta)\dot{\epsilon}^\theta + k_1^\theta k_2^\theta \epsilon^\theta \tag{11}$$

The existence condition of sliding mode are

$$\begin{aligned} \lim_{\sigma^\theta \to +0} \dot{\sigma}^\theta &< 0 \\ \lim_{\sigma^\theta \to -0} \dot{\sigma}^\theta &> 0 \end{aligned} \tag{12}$$

and the time derivative of Eq. (11) contains $\ddot{\theta}$ and $\dot{\omega}_{mr}$ terms, which are substituted by Eq. (8) and (9). Hence, the law of elevation angle tracking is proposed as

$$V_m = \frac{-M_m sign(\sigma^\theta) + V_{mg}}{|\omega_{mr}|} + V_{d\theta}$$
$$V_{mg} = \frac{(k_1^\theta + k_2^\theta) R_m I_{mr}}{2K_{am} K_{Mm}} mgl \sin\theta_d \tag{13}$$

where M_m is the switch gain. It may be possible to show, if k_1^θ and k_2^θ are properly chosen, the present dynamics system is asymptotically stable satisfying Eq. (12).

The last term in Eq. (13), $V_{d\theta}$ is added as a pitch damping control: see Eq. (7). The nominal gravitational torque control V_{mg} will serve to compensate the gravitational torque T_g, which is the major effort to make an elevation angle the desired θ_d. And, the term $M_m/|\omega_{mr}|$ can be said a kind of variable gain because the control voltage V_m is divided by the speed variable ω_{mr}.

The second equation in (13) can be simply written as

$$V_{mg} = K_{g\theta} mgl \sin\theta_d \tag{14}$$

where the $K_{g\theta}$ is a tuneable overall gain, which may be adjusted manually.

The Compensator for the Reaction Torque

Major driving force in the yaw direction is the reaction torque generated by the main rotor shaft, and the tail rotor should keep counteracting to it. The value of reaction torque T_R equals approximately the difference between motor driving torque and friction loss, or $T_{Mm} - T_{fm}$ in the hovering. Neglecting other terms like friction and back-emf effect, the reaction torque (rotor speed ω_{mr} also) is almost proportional to the voltage input of motor, V_m. This fact is also shown in Fig. 3 where the plotted points are measured values in the steady state. Hence, the reaction torque compensator is proposed as

$$V_{R\varphi} = -K_R V_m \tag{15}$$

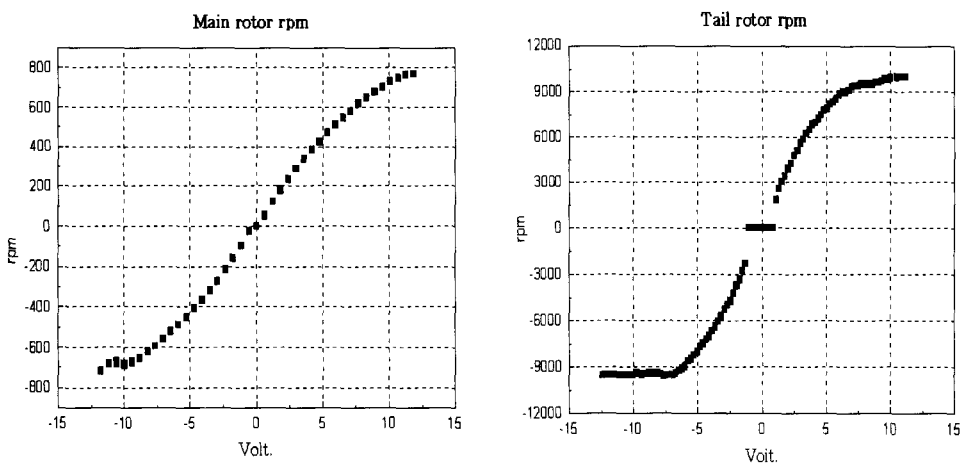

Fig. 3. Voltage-rpm relation: (left) main rotor, (right) tail rotor

Azimuth Angle Tracking Controller

The azimuth direction dynamics can be analyzed like Eq. (3). By the similar procedure, we can derive a sliding mode control equation, which are essentially the same form of Eq. (10) and (11). The resultant control equation is

$$V_t = \left(-\frac{M_t sign(\sigma^{\varphi})}{|\omega_{tr}|} + V_{R_{\varphi}}\right)\sin\theta \tag{16}$$

where M_t is a constant gain, and the divided and multiplied terms $|\omega_{tr}|$ and $\sin\theta$ act as variable gains. The speed ω_{tr} versus a given V_t is shown in Fig. 3.

Experiment and Identification of Parameters

Experimental apparatus was set up for the 2-DOF helicopter model: see Fig. 1. Total mass of the model is 750 g without the supporting post. The diameter of main and tail rotors are 200 to 115 mm, respectively. In the conventional helicopters, the size of tail rotor is about 1/6 of the main rotor, but the yaw dynamics is far exaggerated in this simplified model. Input signal passes through PWM amplifier of 50 μs carrier period. Nominal voltages of main and tail motors range ± 12 V to ± 6 V, respectively. Elevation (pitch) and azimuth (yaw) angles are converted by two encoders of full range, 0 to 65535, which effects on the precision of angle. Angular rate and acceleration signals are obtained by mathematical manipulation. This control algorithm is implemented on a Pentium PC using SIMULINK environment supported by MATLAB^{TM}. The sampling time is 15 ms, which is chosen for this control system. Fig. 4. is the block diagram of the present system.

In Fig. 3, the rotational angular speed of rotors are measured with an portable optical tachometer. The gravitational torque T_g is measured by attaching a known counteracting additional mass in the fuselage on the opposite side from the center of gravity (near the tail rotor). The main and tail rotor torques are obtained with the mass balance method, and the result is shown in Fig. 5.

By the combination of the data plotted in Fig. 4 and Fig. 5, the angular speed and torque relation is obtained in Fig. 6. The identified constants from Fig. 6 are the following gain values:

$$K_{qm} = 2.1784 \times 10^{-7} Nms^2$$

$$K_{qt} = 4.2090 \times 10^{-8} Nms^2 \quad (positive)$$

$$6.3367 \times 10^{-8} Nms^2 \quad (negative)$$

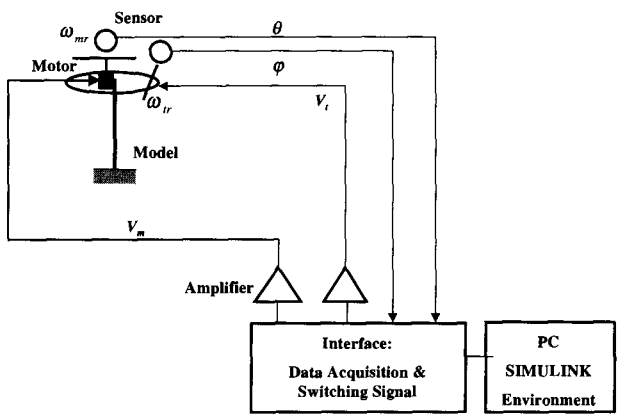

Fig. 4. Block diagram for the experiment

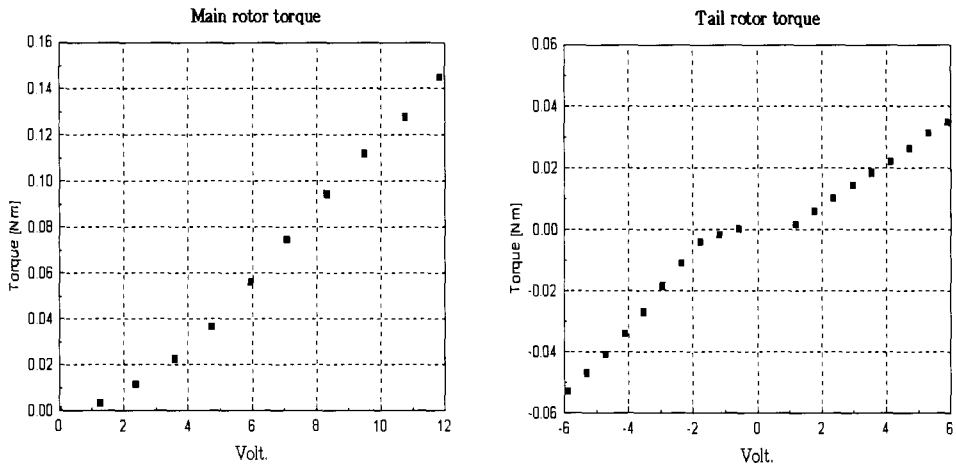

Fig. 5. Voltage-torque relation: (left) main rotor, (right) tail rotor

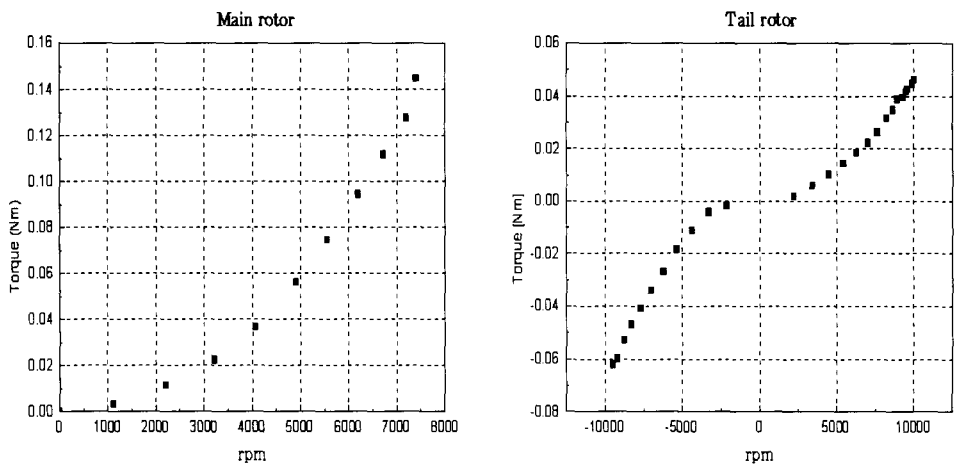

Fig. 6. Speed-torque relation: (left) main rotor, (right) tail rotor

For two rotors, coil resistance R_i can be simply measured by a multimeter, and the constants K_{Mi} and K_{bi} can be acquired form the additional fact, $K_{bi} = K_{Mi}$ and the steady-state test result of speed voltage data without blades.

Aerodynamic coefficients B_{ai} and D_{ai} are obtained from the following algebraic equation derived from the steady state of Eq. (4)-(6), setting $\dot{\omega}_{ir} = 0$.

$$D_{ai}\omega_{ir}^2 + \left(\frac{K_{Mi}K_{bi}}{R_i} + B_{ir} + B_{ai}\right)\omega_{ir} + C_{ir} = \frac{K_{Mi}V_i}{R_i} \tag{17}$$

The above equations are solved for main and tail rotor simultaneously. The coefficients are experimentally fixed in Fig. 3 for the given voltage-speed relation.

Mass moment of inertia in two directions (pitch and yaw) are measured by tri-filar suspension method using the following equation

$$I = \frac{T^2 mgr^2}{4\pi^2 L} \tag{18}$$

where T is oscillating period, r and L are radius and length of tri-filar hanger. The resulting inertias are

$$I_\theta = I_y = 4.08 \times 10^{-3} \quad kg\,m^2$$
$$I_z = 4.06 \times 10^{-3} \quad kg\,m^2$$

Gyroscopic effect is induced by the helicopter rotation in the azimuth direction. By dynamic consideration, the measured value of gyroscopic coefficient while the helicopter rotating is

$$K_G = 3.30 \times 10^{-4} \quad N\,m\,s^2$$

Result and Discussion

Several parameters in the control laws of Eq. (13) and (16) are tuned in series by test as follows. For the pitch damper, sinusoidal disturbance

$$V_m = 6.4 + 0.25 \sin t \quad volts$$

is intensionally loaded to the main motor. This forced oscillation is closed-loop controlled with the feed-back voltage $V_{d\theta}$, and the damper gain $K_{d\theta}$ is tuned from zero to $4.24e+4$ volts. The time history of elevation angle is plotted in Fig. 7. In the zero gain case, the reason of additional disturbance may be regarded as the instability of vertical flight. According to the rotorcraft aerodynamics, the climbing helicopter is accelerated excessively by the increasing motor power, and the descending one experiences a vortex ring region around the rotor. Therefore, there is some unstable region in the vertical flight where the climbing or descending velocity is nonlinear: see the textbook of Newman (1994). When the pitch damper gain is tuned to a proper value, it can be seen in Fig. 7 that the elevation angle becomes uniformly sinusoidal and vertical flight is stabilized. Then, the control gain of nominal gravity $K_{g\theta}$ is tuned from the system parameters obtained in the previous section.

The gain tuning in the pitch direction is performed with a fixed yaw using the azimuth angle controller. The more rigidly the corresponding sliding mode is enforced by increasing the switching gain M_m, the more frequently we observed a high-frequency vibration in the main rotor can occur. This undesirable chattering phenomenon is typical when the sliding mode control with switching function $sign(\sigma^\theta)$ is used in control input. This chattering in turn causes excitation of unmodelled dynamics and high-frequency aeroelastic vibration of blades. Therefore, the steep discontinuity in the switching function is smoothed to a sigmoid function $\tanh(h\sigma)$ where h is adjustable gain: see Jeong and Utkin (1999). Although it sacrifices the invariance

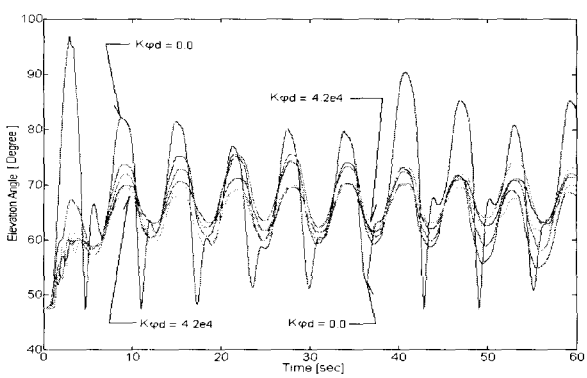

Fig. 7. Pitch oscillation for a given input voltage

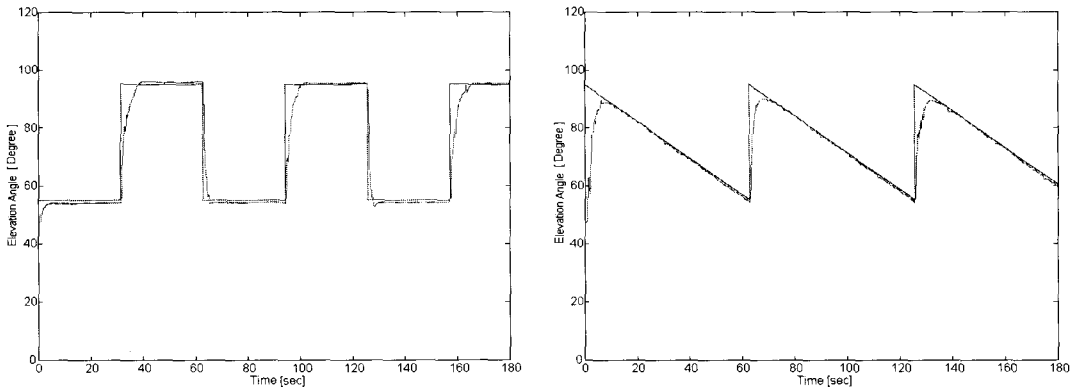

(a) Square form reference signal (b) Saw-tooth form reference signal

Fig. 8. Pitch tracking control result for given signals

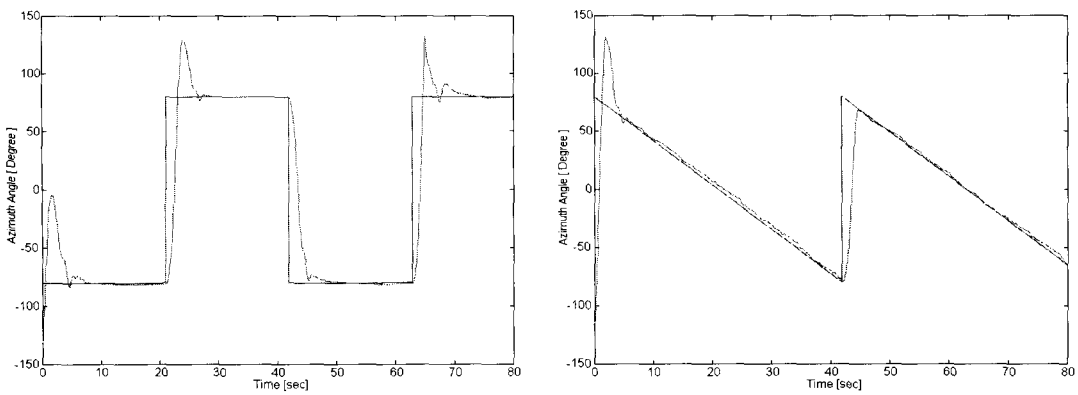

(a) Square form reference signal (b) Saw-tooth form reference signal

Fig. 9. Yaw tracking control result for given signals

property of the sliding mode, the harmful flutter can be removed while the system still maintains robustness. After tuning several times, the experimentally obtained gains are

$$M_m = 2800\ volts$$
$$h^\theta = 0.45\ s^2$$
$$k_1^\theta = 2.0\ Hz,\ k_2^\theta = 2.2\ Hz$$

The elevation (pitch) angle trajectory under the control of Eq. (13) is shown in Fig. 8. The desired wave form is given in square and saw tooth shape, and this control system has a very good tracking performance for the given wave form with fairy small switching gain.

For the azimuth control, the gain for the reaction torque compensator is initially tuned as

$$K_R = 0.395$$

While applying sinusoidal voltage into main motor, the helicopter is moved in the pitch direction, and the control gains in Eq. (16) are chosen

$$M_t = 3250\ volts$$
$$h^\varphi = 0.35\ s^2$$
$$k_1^\varphi = 1.8\ Hz,\ k_2^\varphi = 2.3\ Hz$$

where the helicopter model keeps constant azimuth angle in the yaw direction.

The result of azimuth angle tracking is illustrated in Fig. 9. By the present control system, we achieved the accurate tracking performance with small error and fast response. The overshoot in the wave form is due to the fact that there is no damper in the yaw direction. Contrarily, for the pitch direction in Fig. 8, the pitch damper is working well in the transient motion. The reaction torque is compensated simply in Eq. (15) without closed-loop voltage, and the yaw performance in Fig. 9 seems worse than that of elevation angle comparing with Fig. 8.

Conclusions

Trim and attitude control of a simplified 2-DOF rigid-rotor helicopter model is designed in this paper, and the control system is tested experimentally. Parameters are obtained by means of experimental procedure, and the pitch and yaw control law are based on the sliding mode theory.

In the pitch control, pitch damper and nominal compensator for the gravitational torque is inserted for the desired elevation angle. In the yaw tracking control, we used a reaction torque compensator. The control result shows that the proposed sliding mode tracking works well in the experimental environment, and this control method counteracts several cross-coupling terms physically interpreted as nonlinear and uncertain parameters. Even though the present reduced DOF model differs from the real helicopter, the control algorithm is expected to apply to the tracking control of conventional 6-DOF rotorcraft.

References

1. Prouty, R. W., 1986, *Helicopter performance, stability, and control,* PWS Publishers, Boston, pp. 541-637.

2. Newman, S., 1994, *The foundation of helicopter flight*, Edward Arnold, London.

3. Parry, D. L. K. and Murray-Smith, D. J., 1985, "The application of modal control theory to the single rotor helicopter", *Proc. 11th European Rotorcraft Forum,* London, September.

4. Mannes, M. A., Gribble, J. J. and Murray-Smith, D. J., 1990, "Multivariable methods for helicopter flight control law design: a review", *Proc. 16th Annual Society European Rotorcraft Forum,* Glasgow, Scotland, September.

5. Postlethwaite I. and Walker, D. J., 1994, "The design of the helicopter control systems using advanced H_∞ control", *Proc. American Control Conference,* Baltimore, June, pp. 3193-3197.

6. Jeong, H. S. and Utkin, V. I., 1999, "Sliding mode tracking control of systems with unstable zero dynamics", *Variable structure systems, sliding mode and nonlinear control, LNCS,* Springer-Verlag, Berlin.

7. Im, K. M. and Ham W. C., 1997, "Sliding mode control for helicopter attitude regulation at hovering", *ICASE Journal,* Vol. 3, No. 3, pp. 563-568.

8. Leishman J., 2000, *Principles of helicopter aerodynamics*, Cambridge University Press.

9. Andrew Y. Ng, Kim H. J. et al., 2004, "Autonomous helicopter flight via reinforcement learning", *NIPS16.*

10. Heon-Sul Jeong, Jin-Sung Park, Seok-Hyung Oh, Jun-Won Yun, 1999, "Sliding Mode Attitude Control of a 2 DOF Model Helicopter", *3rd International Workshop on Advanced Mechatronics*, Chunchon, KOREA.